

${}^3\vec{\text{H}}\text{e}(\text{p},\text{p}){}^3\text{He}$  analyzing powers between 25 and 35 MeV

R. H. McCamis, P. J. T. Verheijen,\* W. T. H. van Oers, P. Drakopoulos, C. Lapointe,<sup>†</sup>  
G. R. Maughan, and N. T. Okumusoglu<sup>‡</sup>

*Department of Physics, University of Manitoba, Winnipeg, Manitoba, Canada R3T 2N2*

Ronald E. Brown

*Los Alamos National Laboratory, Los Alamos, New Mexico 87545*

(Received 28 January 1985)

A polarized  ${}^3\text{He}$  target, which uses conventional optical pumping with  ${}^4\text{He}$  discharge lamps, has been used for the measurement of  ${}^3\text{He}$  analyzing powers  $A_y(\theta)$  at energies of 25.0, 30.0, 32.5, and 35.0 MeV. The statistical uncertainties in the data are on the order of 0.03; the systematic uncertainty is estimated to be 0.05. These data are compared with fits and predictions from various phase shift analyses.

## I. INTRODUCTION

One of the fundamental goals of nuclear physics is to have the ability to describe a many-body nuclear system, i.e., a nucleus, by summing up the individual interactions between, or among, the constituent particles, whether they are nucleons or quarks. With recent advances in the Faddeev three-body formalism<sup>1</sup> yielding impressively good results for three-nucleon systems in many cases,<sup>2</sup> it seems only natural to begin to study the four-nucleon systems in more detail.

The most direct method of studying the four-nucleon configuration of three protons and one neutron, that is to say, the  ${}^4\text{Li}$  nucleus, is via proton- ${}^3\text{He}$  scattering. This is, of course, an unbound nuclear state, with its ground state estimated to be 4.7 MeV above the summed energy of a proton plus a  ${}^3\text{He}$  particle. From low energy ( $T_p \leq 19$  MeV) proton- ${}^3\text{He}$  scattering data, four levels have been deduced.<sup>3</sup> Above these levels, no further structure has been found, although a preliminary  $R$ -matrix analysis<sup>4</sup> indicated fluctuations in certain phase shifts. In addition, knowledge of  $\text{p-}{}^3\text{He}$  phase shifts is directly applicable to the charge-symmetric system, the interaction of a neutron with tritium, assuming the charge symmetry of the nuclear forces. The unstable nature of both of the latter particles makes experiments with them more difficult than similar  $\text{p-}{}^3\text{He}$  experiments are.

A comprehensive set of  $\text{p-}{}^3\text{He}$  elastic scattering observables, specifically the proton and  ${}^3\text{He}$  analyzing powers, as well as the spin correlation parameters  $A_{yy}$  and  $A_{xx}$ , have been measured at 19.4 MeV.<sup>5</sup> A phase shift analysis of these data plus the differential cross section measurements of Morales *et al.*<sup>6</sup> was also performed by Baker *et al.*<sup>5</sup> The availability of extensive spin-dependent data was, of course, essential for the production of a satisfactory phase shift solution.

Spin-dependent data requiring polarized protons can be obtained in a straightforward manner. However, data requiring a polarized  ${}^3\text{He}$  target become increasingly more difficult to obtain beyond 20 MeV, because such targets are restricted to low pressures ( $< 1$  kPa, or a few Torr)

and low polarizations ( $< 0.25$ ) due to the properties of the optical pumping techniques used to date to polarize  ${}^3\text{He}$  nuclei. As the energy increases, the  $\text{p-}{}^3\text{He}$  differential cross sections diminish and background scattering becomes relatively more important. It should be noted that recent developments in laser technology<sup>7,8</sup> may allow these restrictions to be alleviated considerably.

Complete or partial angular distributions of  ${}^3\text{He}$  analyzing powers have been measured between 2.3 and 8.8 MeV,<sup>9</sup> between 3.9 and 10.9 MeV,<sup>10</sup> at 19.4 MeV,<sup>5</sup> at 25.0 MeV,<sup>11</sup> and at 26.8 MeV.<sup>12</sup> In addition, Müller *et al.*<sup>11</sup> have measured  ${}^3\text{He}$  analyzing powers at one angle for five energies between 19.6 and 26.5 MeV. Spin-correlation parameters have been measured only at 8.8 MeV (Ref. 13) and at 19.4 MeV.<sup>5</sup>

Several phase shift analyses of the  $\text{p-}{}^3\text{He}$  system have been performed below 14 MeV.<sup>10,14-19</sup> Other phase shift analyses in the energy region under consideration (below approximately 50 MeV) have been carried out at several energies between 18 and 57 MeV,<sup>6</sup> at 19.4 MeV,<sup>5,20</sup> at 25.0 MeV,<sup>11</sup> at 30.5 MeV,<sup>11,20,21</sup> and at 49.5 MeV.<sup>21</sup>

To advance the study of the  $\text{p-}{}^3\text{He}$  system to higher energies, a substantial program of measurements has been undertaken in the energy range between 20 and 50 MeV. Previous components of this program include measurements of total reaction cross sections,<sup>22</sup> differential cross sections,<sup>23</sup> and proton analyzing powers.<sup>24</sup> (Complete references to previous  $\text{p-}{}^3\text{He}$  elastic scattering studies may be found in Refs. 23 and 24.) This paper reports on the measurement of  ${}^3\text{He}$  analyzing powers at 25.0, 30.0, 32.5, and 35.0 MeV using a polarized  ${}^3\text{He}$  target. The data at 25.0 MeV were taken for comparison with the previous data of Müller *et al.*<sup>11</sup>

## II. EXPERIMENT

The experiment was performed using the University of Manitoba sector focussed cyclotron. Experiments were conducted at proton beam energies of 25.0, 30.0, 32.5, and 35.0 MeV. The incident proton energies were known with an uncertainty of  $\pm 150$  keV from a calibration of the

momentum-analyzing magnetic field using the kinematic crossover method;<sup>25</sup> the energy spread of the proton beam was less than 200 keV full width at half maximum (FWHM). Incident beam currents on the target were normally between 50 and 100 nA; after passing through the target, the beam was collected in an external, well-shielded Faraday cup and integrated using a current integrator.

The polarized  $^3\text{He}$  target used for the experiments has been described fully elsewhere;<sup>26</sup> for completeness, however, a few features are described here. The  $^3\text{He}$  gas was contained in a glass cell at a pressure between 0.15 and 0.65 kPa (approximately 1 to 5 Torr) at the center of a pair of Helmholtz coils, which supplied a weak magnetic field of 4.2 mT. The  $^3\text{He}$  gas was polarized by the optical pumping technique (see Ref. 26 and the references therein) using circularly polarized light at 1083 nm from two  $^4\text{He}$  discharge lamps, one above and one below the target cell (with opposite helicities of light). Polarizations achieved ranged from 0.11 at 0.65 kPa to 0.21 at 0.22 kPa. In this range, the most optimal values<sup>26</sup> were obtained for  $P^2\rho$ , the product of the polarization squared and the target density.

Scattered protons were detected at four angles, each separated by  $10.0^\circ \pm 0.05^\circ$ , simultaneously on either side of the incident beam. The scattering angle could be set to an accuracy of  $0.1^\circ$ . The detection system<sup>26</sup> consisted of  $\Delta E$ - $E$  telescopes of either one surface barrier detector (typically  $200\text{ mm}^2$  in area, 0.2 mm thick) and a NaI detector (38 mm diameter, 13 mm thick) or two silicon surface barrier detectors ( $200\text{ mm}^2$  by 0.1 mm, and  $200\text{ mm}^2$  by 1 mm, respectively), depending on the energy of the elastically scattered protons at that angle. Sets of near-identical collimators (4.8 mm wide by 12.7 mm high, at a radius of 238 mm), with a thickness just sufficient to stop the maximum energy protons, accurately defined the solid angle acceptance of the detection system, approximately 1.08 msr. A similarly sized set of slits at a radius of 51 mm defined the active volume of the gas target.

For the measurements of the analyzing powers at large angles ( $> 90^\circ$ ) at 30 and 35 MeV, two fixed monitor counters, located at  $20^\circ$  on either side of the incident pro-

ton beam direction, viewed the beam exit window of the target cell, to detect elastically scattered protons. A program running on the VAX 11/750 data acquisition computer monitored the ratio of the number of counts in the two detectors as an indication of beam movement at the target. If such a movement was detected, small corrections to the beam transport system were automatically made. For those data acquired at forward angles where the monitor detectors were obscured by the main detection apparatus, the beam position was maintained manually by frequent observations of a scintillation screen placed at the target position.

### III. DATA REDUCTION

The raw data, which were stored on line on magnetic tape for later analysis, were reduced to  $^3\text{He}$  analyzing powers in several steps. The first step in the analysis was to subtract the background from under the elastic scattering peak, to obtain net peak areas. The peak areas thus obtained were then corrected for system dead time and were normalized with respect to the integrated beam current.

Due to the perturbation in the trajectories of the scattered protons caused by the weak Helmholtz field, a complete cycle of measurements consisted of four runs with each possible combination of directions for the target polarization and the magnetic field. Thus, one cycle of measurements produced yields at one angle from left and right detectors in four consecutive runs, i.e., eight peak areas. Analytical expressions for these yields, similar to those used by Baker *et al.*<sup>27</sup> and Szaloky,<sup>28</sup> are given in Table I. The definitions of the symbols used in Table I are as follows:  $n_i$  represents the total number of particles in the beam for run  $i$  ( $i = a, b, c, d$ );  $N$  represents the number of target nuclei per  $\text{m}^3$ ;  $G$  represents the gas scattering geometry factor<sup>29</sup> for either left or right detector;  $\sigma$  represents the differential cross section ( $\text{m}^2$ );  $P_i$  represents the target polarization for run  $i$ ;  $A_y$  represents the analyzing power;  $\theta$  represents the actual scattering angle, in the laboratory system, at which the analyzing power is to be

TABLE I. Formulae defining the yields in the determination of nuclear scattering asymmetries (see the text for an explanation of the symbols). These formulae are similar to those used by Baker *et al.* (Ref. 27) and by Szaloky (Ref. 28).

Run	Target polarization	Magnetic field	Yield
Left detector			
<i>a</i>	up	up	$Y_1 = n_a N G_L(\theta_L + \Delta\theta)\sigma(\theta_L + \Delta\theta)[1 + P_a A_y(\theta_L + \Delta\theta)]$
<i>b</i>	down	up	$Y_2 = n_b N G_L(\theta_L + \Delta\theta)\sigma(\theta_L + \Delta\theta)[1 - P_b A_y(\theta_L + \Delta\theta)]$
<i>c</i>	down	down	$Y_3 = n_c N G_L(\theta_L - \Delta\theta)\sigma(\theta_L - \Delta\theta)[1 - P_c A_y(\theta_L - \Delta\theta)]$
<i>d</i>	up	down	$Y_4 = n_d N G_L(\theta_L - \Delta\theta)\sigma(\theta_L - \Delta\theta)[1 + P_d A_y(\theta_L - \Delta\theta)]$
Right detector			
<i>a</i>	up	up	$Y_5 = n_a N G_R(\theta_R - \Delta\theta)\sigma(\theta_R - \Delta\theta)[1 - P_a A_y(\theta_R - \Delta\theta)]$
<i>b</i>	down	up	$Y_6 = n_b N G_R(\theta_R - \Delta\theta)\sigma(\theta_R - \Delta\theta)[1 + P_b A_y(\theta_R - \Delta\theta)]$
<i>c</i>	down	down	$Y_7 = n_c N G_R(\theta_R + \Delta\theta)\sigma(\theta_R + \Delta\theta)[1 + P_c A_y(\theta_R + \Delta\theta)]$
<i>d</i>	up	down	$Y_8 = n_d N G_R(\theta_R + \Delta\theta)\sigma(\theta_R + \Delta\theta)[1 - P_d A_y(\theta_R + \Delta\theta)]$

measured (and also the detector's angular position); and  $\Delta\theta$  represents the small change in the scattering angle caused by the protons traversing the target's magnetic field. Therefore,  $\theta \pm \Delta\theta$  is the angle at which a proton must have been scattered in order to enter the detection system along its central axis, given a finite magnetic field. The change in scattering angle  $\Delta\theta$  may be calculated from a knowledge of the momentum of the proton and the magnetic field strength. Typically, it is of the order of  $0.15^\circ$  at 30 MeV. The angular arguments ( $\theta_L$  and  $\theta_R$ ) allow for possible left-right differences in the scattering angle due to geometrical asymmetries in the apparatus, or due to nonideal beam transport through the target cell.

Such differences will appear as an instrumental asymmetry  $\epsilon_i$  (see below). The final data are quoted for the mean of  $\theta_L$  and  $\theta_R$ . The gas scattering geometry factor  $G$  may be expressed<sup>29</sup> as

$$G(\theta) = \frac{A_r w_f}{h R_r \sin(\theta)},$$

where  $A_r$  represents the area of the rear aperture (in  $\text{m}^2$ );  $w_f$  represents the width of the front aperture (in m);  $h$  represents the distances between the front and rear apertures (in m); and  $R_r$  represents the distance from the target center to the rear aperture (in m). The equations of

TABLE II. Measured values of  ${}^3\text{He}$  analyzing powers from 25.0 to 35.0 MeV. The analyzing powers have a normalization uncertainty ( $\Delta P/P$ ) of 5%, in addition to the stated relative errors (see the text for details).

Proton laboratory energy (MeV)	Laboratory angle (deg)	Center of mass angle (deg)	Analyzing power
25.0	40.0	52.6	$-0.089 \pm 0.025$
	50.0	65.1	$-0.129 \pm 0.023$
	60.0	77.1	$-0.177 \pm 0.025$
	70.0	88.6	$-0.226 \pm 0.042$
	80.0	99.5	$-0.248 \pm 0.092$
	90.0	109.8	$-0.10 \pm 0.15$
30.0	30.0	39.8	$-0.069 \pm 0.042$
	40.0	52.7	$-0.061 \pm 0.018$
	50.0	65.1	$-0.175 \pm 0.025$
	60.0	77.1	$-0.236 \pm 0.026$
	70.0	88.6	$-0.219 \pm 0.038$
	80.0	99.5	$-0.337 \pm 0.091$
	90.0	109.8	$-0.096 \pm 0.053$
	100.0	119.5	$0.182 \pm 0.064$
	110.0	128.6	$0.452 \pm 0.036$
	120.0	137.0	$0.331 \pm 0.033$
	130.0	145.0	$0.184 \pm 0.028$
140.0	152.6	$0.082 \pm 0.044$	
32.5	30.0	39.8	$-0.054 \pm 0.024$
	40.0	52.7	$-0.062 \pm 0.020$
	50.0	65.2	$-0.134 \pm 0.024$
	60.0	77.2	$-0.198 \pm 0.025$
	70.0	88.7	$-0.233 \pm 0.026$
	80.0	99.6	$-0.219 \pm 0.041$
	90.0	109.9	$-0.136 \pm 0.063$
	100.0	119.5	$0.25 \pm 0.10$
35.0	30.0	39.9	$-0.034 \pm 0.019$
	40.0	52.7	$-0.085 \pm 0.019$
	50.0	65.2	$-0.134 \pm 0.026$
	60.0	77.2	$-0.217 \pm 0.030$
	70.0	88.7	$-0.238 \pm 0.034$
	80.0	99.6	$-0.271 \pm 0.054$
	90.0	109.9	$-0.131 \pm 0.036$
	100.0	119.5	$0.155 \pm 0.055$
	110.0	128.6	$0.397 \pm 0.039$
	120.0	137.1	$0.323 \pm 0.035$
	130.0	145.1	$0.205 \pm 0.033$
140.0	152.6	$0.194 \pm 0.040$	

Table I may be rewritten in terms of the magnetic field related asymmetry  $\epsilon_m$ , an instrumental asymmetry  $\epsilon_i$ , and the nuclear scattering asymmetry  $\epsilon_n$  ( $\epsilon_n = P_i A_y$ ) as

$$Y_j = k(1 \pm \epsilon_m)(1 \pm \epsilon_i)(1 \pm \epsilon_n), \quad j = 1, 8,$$

where  $k$  is a constant, and where the signs are determined by the direction of the magnetic field, the choice of left or right detector, and the direction of the target polarization, respectively. [It should be noted that, due to the target polarizations  $P_i$  being of the order of 0.15–0.20, and the measured analyzing powers  $A_y$  being less than 0.40 (see below), the nuclear scattering asymmetry  $\epsilon_n$  was of the order of a few percent, the same general magnitude as both the magnetic field and instrumental asymmetries.] These eight equations were solved for the magnetic field and instrumental asymmetries and the analyzing powers; as well, various tests of the internal consistency of the data were made.<sup>27,30</sup> The magnetic field related asymmetry was estimated, using the quantity  $\Delta\theta$  (see above) and the slope of the differential cross section at that angle; in general, the calculated and experimental values for  $\epsilon_m$  were in good agreement. Finally, the analyzing power results at a given angle for all measurement cycles were combined and a weighted average was calculated.

#### IV. EXPERIMENTAL RESULTS AND DISCUSSION

The experimental results are listed in Table II and are shown in Figs. 1 and 2. The relative errors in the data are given, and are dominated by counting statistics, with considerably smaller contributions coming from uncertainties in the target polarization measurement, beam current integration, and in the determination of the scattering angle.<sup>30</sup> Further, there is a normalization uncertainty in the target polarization ( $\Delta P/P$ ) of 5%.<sup>26</sup> The measurement method is such that all magnetic field related and instrumental asymmetries are effectively eliminated to at least the first order in their magnitudes. Any residual second-order effects would be negligibly small, compared to the

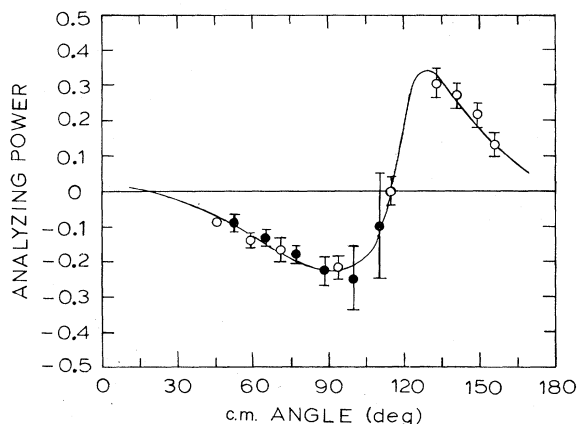


FIG. 1. A comparison of the present analyzing power data at 25 MeV (full circles) with the previous data of Müller *et al.* (Ref. 11) (open circles). The smooth curve is the result of a phase shift analysis (see the text for details).

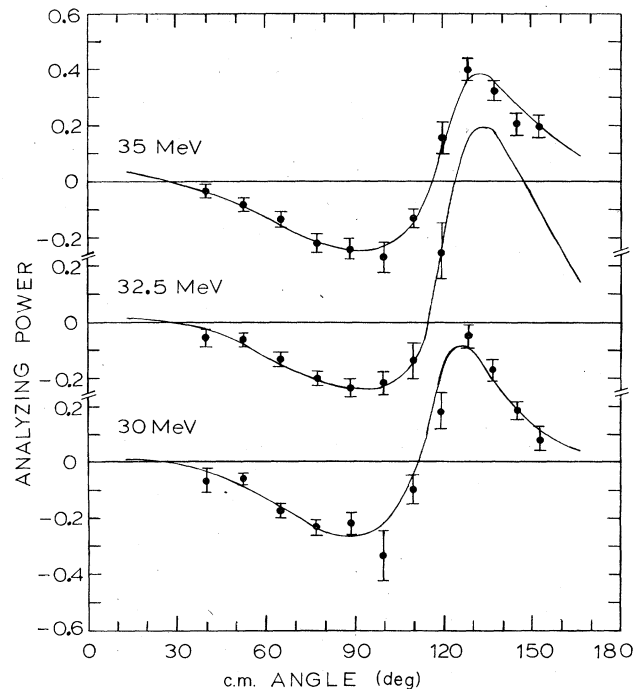


FIG. 2. The present  $^3\text{He}$  analyzing powers at 30, 32.5, and 35 MeV. The smooth curves are the results of a phase shift analysis (see the text).

other uncertainties previously mentioned.

As stated in the Introduction, the  $^3\text{He}$  analyzing powers have been previously measured at 25.0 MeV.<sup>11</sup> In order to verify the current experimental procedures, we have also measured a limited number of analyzing powers at this energy. A comparison of these two data sets, presented in Fig. 1, shows good agreement.

Data at the remaining energies are presented in Fig. 2. These data and those at 19.4 MeV,<sup>5</sup> 25.0 MeV,<sup>11</sup> and 26.8 MeV (Ref. 12) may be seen to be quite similar. Further, a comparison of the present  $^3\text{He}$  analyzing powers with the proton analyzing powers of Ref. 24 shows that the two observables are qualitatively quite similar, that is to say, negative analyzing powers at forward angles, changing sign at  $\theta_{\text{c.m.}} \sim 120^\circ$  to somewhat larger, positive analyzing powers at backward angles. Overall, however, the proton analyzing powers are larger in magnitude by almost a factor of 2. Such differences are found to be proportional to those matrix elements which describe the spin singlet-spin triplet mixing in the partial waves.

Previous phase shift results of the  $p + ^3\text{He}$  system between 19 and 30 MeV,<sup>6,20</sup> predicted<sup>11,12</sup> large variations with energy for the  $^3\text{He}$  analyzing powers. The previous data at 25 (Ref. 11) and 26.8 MeV (Ref. 12) did not support these predictions, but the present data, extending from 25 to 35 MeV, demonstrate conclusively that the analyzing powers do not permit such variations with energy. The phase-shift analysis<sup>4,23</sup> which used the  $R$ -matrix parametrization,<sup>31</sup> but did not include any polarized  $^3\text{He}$  data, predicts only a limited variation of the  $^3\text{He}$  analyzing power over this energy range, in qualitative agreement

with the present experiment. However, this analysis yields a significantly larger minimum-to-maximum excursion of the analyzing power as a function of angle than is given by experiment. For example, at 30 MeV this analysis yields an analyzing power variation from about  $-0.6$  to  $+0.6$ , whereas the experiment shows a variation from  $\approx -0.3$  to  $+0.45$ .

The  ${}^3\text{He}$  analyzing powers presented herein have been used as input to a single energy phase shift analysis,<sup>30</sup> together with previous total reaction cross sections,<sup>22</sup> differential cross sections,<sup>23</sup> proton analyzing powers,<sup>24</sup> the  ${}^3\text{He}$  analyzing powers at 25.0 (Ref. 11) and 26.8 MeV,<sup>12</sup> and the spin correlation data at 19.4 MeV.<sup>5</sup> Partial waves up to  $L=4$ , including complex phases to  $L=3$ , were allowed in the analysis. The results of these fits are plotted as solid lines in Figs. 1 and 2, and are seen to provide an

excellent representation of the data. The inclusion of the higher partial waves and a more complete set of inelasticity parameters, as compared with previous phase shift analyses (see Sec. I), improved the fits significantly. Complete details and results of the phase shift analysis will appear in a later publication.<sup>32</sup>

#### ACKNOWLEDGMENTS

The authors would like to thank Carleen de Wit for her valuable assistance in the analysis of the data. This work was supported in part by the Natural Sciences and Engineering Research Council of Canada, the University of Manitoba Research Grants Committee, and the U. S. Department of Energy.

\*Present address: Natuurkundig Laboratorium, Vrije Universiteit, Amsterdam, the Netherlands.

†Present address: Nuclear Research Centre, University of Alberta, Edmonton, Alberta, Canada T6G 2N5.

‡Permanent address: Department of Physics, 19 Mayıs University, Samsun, Turkey.

<sup>1</sup>L. D. Fadeev, Zh. Eksp. Teor. Fiz. **39**, 1459 (1960) [Sov. Phys.-JETP **12**, 1014 (1961)]; P. Doleschall, Nucl. Phys. **A201**, 264 (1973).

<sup>2</sup>J. E. Simmons, in *Few Body Problems in Physics*, in Proceedings of the Tenth International Conference on Few Body Problems in Physics, edited by B. Zeitnitz, Nucl. Phys. **A416**, 553c (1984), and references therein.

<sup>3</sup>S. Fiarman and W. E. Meyerhof, Nucl. Phys. **A206**, 1 (1973).

<sup>4</sup>R. E. Brown, in *Clustering Aspects of Nuclear Structure and Nuclear Reactions (Winnipeg, 1978)*, Proceedings of The Third International Conference on Clustering Aspects of Nuclear Structure and Nuclear Reactions, AIP Conf. Proc. No. 47, edited by W. T. H. van Oers, J. P. Svenne, J. S. C. McKee, and W. R. Falk (AIP, New York, 1978), p. 90.

<sup>5</sup>S. D. Baker, T. A. Cahill, P. Catillon, J. Durand, and D. Garreta, Nucl. Phys. **A160**, 428 (1971).

<sup>6</sup>J. R. Morales, T. A. Cahill, D. J. Shadoan, and H. Willmes, Phys. Rev. C **11**, 1905 (1975).

<sup>7</sup>L. F. Mollenauer, Opt. Lett. **5**, 188 (1980).

<sup>8</sup>P. J. Nacher, M. Leduc, G. Tréneç, and F. Laloë, J. Phys. Lett. (Paris) **43**, L525 (1982).

<sup>9</sup>G. Szaloky, F. Seiler, W. Gruebler, and V. König, Nucl. Phys. **A303**, 51 (1978).

<sup>10</sup>D. H. McSherry and S. D. Baker, Phys. Rev. C **1**, 888 (1970).

<sup>11</sup>D. Müller, R. Beckmann, and U. Holm, Nucl. Phys. **A311**, 1 (1978).

<sup>12</sup>R. H. Ware, W. R. Smythe, and P. D. Ingalls, Nucl. Phys. **A242**, 309 (1975).

<sup>13</sup>D. H. McSherry, S. D. Baker, G. R. Plattner, and T. B. Clegg, Nucl. Phys. **A126**, 233 (1969).

<sup>14</sup>T. A. Tombrello, Phys. Rev. **138**, B40 (1965).

<sup>15</sup>L. Drigo and G. Pisent, Nuovo Cimento **51B**, 419 (1967); L. Beltramin, R. Del Frate, and G. Pisent, in *Few Body Problems*

in *Physics*, in *Proceedings of the Tenth International Conference on Few Body Problems in Physics*, edited by B. Zeitnitz (Elsevier, Amsterdam, 1984), Vol. II, p. 421.

<sup>16</sup>L. W. Morrow and W. Haeblerli, Nucl. Phys. **A126**, 225 (1969).

<sup>17</sup>G. M. Hale, J. J. Devaney, D. C. Dodder, and K. Witte, Bull. Am. Phys. Soc. **19**, 506 (1974).

<sup>18</sup>G. Szaloky and F. Seiler, Nucl. Phys. **A303**, 57 (1978).

<sup>19</sup>H. Berg, W. Arnold, E. Huttel, H. H. Krause, J. Ulbricht, and G. Clausnitzer, Nucl. Phys. **A334**, 21 (1980).

<sup>20</sup>R. Darves-Blanc, Nguyen Van Sen, J. Arvieux, J. C. Gondrand, A. Fiore, and G. Perrin, Nucl. Phys. **A191**, 353 (1972).

<sup>21</sup>S. A. Harbison, R. J. Griffiths, N. M. Stewart, A. R. Johnston, and G. T. A. Squier, Nucl. Phys. **A150**, 570 (1970).

<sup>22</sup>A. M. Sourkes, A. Houdayer, W. T. H. van Oers, R. F. Carlson, and R. E. Brown, Phys. Rev. C **13**, 451 (1976).

<sup>23</sup>B. T. Murdoch, D. K. Hasell, A. M. Sourkes, W. T. H. van Oers, P. J. T. Verheijen, and R. E. Brown, Phys. Rev. C **29**, 2001 (1984).

<sup>24</sup>J. Birchall, W. T. H. van Oers, J. W. Watson, H. E. Conzett, R. M. Larimer, B. Leemann, E. J. Stephenson, P. von Rossen, and R. E. Brown, Phys. Rev. C **29**, 2009 (1984).

<sup>25</sup>B. M. Bardin and M. E. Rickey, Rev. Sci. Instrum. **35**, 902 (1964); R. Smythe, *ibid.* **35**, 1197 (1964).

<sup>26</sup>P. J. T. Verheijen, R. H. McCamis, P. Drakopoulos, W. T. H. van Oers, J. M. Daniels, and A. D. May, Nucl. Instrum. Methods **227**, 71 (1984).

<sup>27</sup>S. D. Baker, D. H. McSherry, and D. O. Findley, Phys. Rev. **178**, 1616 (1969).

<sup>28</sup>G. Szaloky, Ph.D. thesis, University of Basel, Basel, Switzerland, 1975 (unpublished).

<sup>29</sup>E. A. Silverstein, Nucl. Instrum. Methods **4**, 53 (1959).

<sup>30</sup>P. J. T. Verheijen, Ph.D. thesis, University of Manitoba, Winnipeg, Canada, 1983 (unpublished).

<sup>31</sup>A. M. Lane and R. G. Thomas, Rev. Mod. Phys. **30**, 257 (1958).

<sup>32</sup>P. J. T. Verheijen, R. H. McCamis, and W. T. H. van Oers (unpublished).